Metallaheteroborane Chemistry. Part 12.[1] Synthesis of Cationic Metallaheteroboranes [2-L-2-(PPh_3)-*closo*-2,1-$PdTeB_{10}H_9(PPh_3)$][BF_4]; Molecular Structures of the Compounds with L = H_2O or CO†

James P. Sheehan,[a] Trevor R. Spalding,*[,a] George Ferguson,*[,b] John F. Gallagher,[b] Branko Kaitner[b] and John D. Kennedy[c]
[a] *Chemistry Department, University College, Cork, Ireland*
[b] *Chemistry Department, University of Guelph, Guelph, Ontario N1G 2W1, Canada*
[c] *School of Chemistry, University of Leeds, Leeds LS2 9JT, UK*

The reaction of Ag[BF_4] and [2-I-2-(PPh_3)-*closo*-2,1-$PdTeB_{10}H_9(PPh_3)$] **1** in toluene for 30 min at room temperature and subsequent isolation of the product under aerobic conditions afforded [2-(H_2O)-2-(PPh_3)-*closo*-2,1-$PdTeB_{10}H_9(PPh_3)$][BF_4] **2** in excellent yield. This complex has been characterised by (IR and ^{11}B NMR) spectroscopy and X-ray crystallography. Crystals of **2**·$0.89CH_2Cl_2$ are monoclinic, space group $P2_1/c$, with cell dimensions a = 14.073(3), b = 15.640(2), c = 20.262(6) Å and β = 94.80(2)°. A final R factor of 0.038 was calculated for 5595 observed reflections. The Pd–OH_2 distance is 2.208(4) Å and Pd–P(1) is 2.3544(14) Å. Cage interatomic distances include Pd–Te 2.6958(6) and ranges for Pd–B of 2.192(6)–2.299(6) and Te–B of 2.287(6)–2.403(6) Å. The *exo*-cage B(7)–P(2) distance is 1.950(6) Å. The water molecule in **2** can be displaced by a variety of ligands to produce the cationic pallada-telluraborane complexes [2-L-2-(PPh_3)-*closo*-2,1-$PdTeB_{10}H_9(PPh_3)$][BF_4] [L = CO, CNBu^t, CNC_6H_{11}, NCMe, MeCH(Ph)NH_2, OC_4H_8 or SC_4H_8) in yields ranging from 39 to 93%. Reaction between **2** and a ten-fold excess of PMe_2Ph affords [2,2-$(PMe_2Ph)_2$-*closo*-2,1-$PdTeB_{10}H_9(PPh_3)$][BF_4] in 75% yield. All complexes have been characterised spectroscopically (IR and ^{11}B NMR) and in the case of [2-(CO)-2-(PPh_3)-*closo*-2,1-$PdTeB_{10}H_9(PPh_3)$][BF_4] **3** by X-ray crystallography. The **3**·C_6H_5Me solvate crystallises in the monoclinic space group $P2_1/c$ with Z = 4, a = 14.509(3), b = 10.732(1), c = 31.377(8) Å and β = 97.49(2)°. The final R factor of 0.054 was calculated from 5439 observed reflections. Principal interatomic distances include Pd–Te 2.6897(9), Pd–B 2.195(10)–2.307(9), Te–B 2.262(11)–2.389(9), Pd–P(2) 2.367(2), B(11)–P(1) 1.941(9) and Pd–C(1) 2.003(9) Å.

Virtually all the metallaboranes and metallaheteroboranes which have been described are either neutral or anionic.[2] The very few cationic compounds which are known include *nido*-[$Fe(CO)_3(B_5H_9)$]$^+$ (ref. 2) and [1-(η^5-C_5H_5)-7-(C_5H_5N)-*closo*-1,2,4-$CoC_2B_8H_9$]$^+$.[3] The former was unstable above −30 °C and the latter decomposed within a few hours at room temperature when dissolved in polar solvents. The preparation of these compounds involved either the protonation of the borane cage[3] or the removal of a hydride ion from a μ-B–H–M fragment.[4] An alternative approach to cationic compounds was reported with the electrochemical oxidation of [*commo*-3,3′-Fe{3,1,2-$FeC_2B_9H_{10}(SEt_2)$}$_2$].[5] However, the iron(III) complex cation, isolated as the perchlorate salt, defied all attempts to purify it and work on this complex ceased. More recently, Kang *et al.*[5] reported the synthesis of [*commo*-3,3′-Co{4-[4-($MeCO_2$)C_5H_4N]-3,1,2-$CoC_2B_9H_{10}$}$_2$]Cl from the reaction between $CoCl_2$ and [*nido*-9-{4-($MeCO_2$)C_5H_4N}-7,8-$C_2B_9H_{11}$]$^-$ in thf. Since the chloride complex was relatively unstable, a salt was prepared with the [*nido*-7,8-$C_2B_9H_{12}$]$^-$ anion. Both these compounds were characterised by spectroscopic methods but no crystallographic studies were reported. One of the conclusions of this study was that the instability of the cobaltacarborane cation was due to the presence of the positive charge.[6]

In continuation of our study of transition-metal complexes of heteroborane ligands,[1] we now report the use of metal-centred chemistry to synthesise a series of nine, air-stable, cationic metallaheteroboranes with the general formula [2-L-2-(PPh_3)-*closo*-2,1-$PdTeB_{10}H_9(PPh_3)$][BF_4] where L = H_2O, CO, Bu^{t}NC, $C_6H_{11}NC$, MeCN, MeCH(Ph)NH_2, tetrahydrothiophene (tht), or tetrahydrofuran (thf), compounds **2**–**9** and [2,2-$(PMe_2Ph)_2$-*closo*-2,1-$PdTeB_{10}H_9(PPh_3)$][BF_4] **10**. All these products were characterised by analytical and spectroscopic data. Generally in this paper we describe the 7-(PPh_3) enantiomer for convenience; both 7 and 11 enantiomers are present in the racemic products.

Prior to this report, only two mononuclear palladium complexes containing Pd–OH_2 moieties had been structurally characterised, namely, aqua(benzo[*h*]quinoline)[2-(dimethylaminomethyl)phenyl-*N*]palladium(II) perchlorate, [Pd(bquin)(dmp)(H_2O)][ClO_4] **11**[7] and aqua(1-methyl-2,2′-bipyridin-3-ylium-κC^3,$N^{1'}$)(nitrato-κ*O*)palladium(II) perchlorate monohydrate, [PdL′(H_2O)(ONO_2)][ClO_4]·H_2O **12**.[8] Furthermore, structural studies of mononuclear Pd(CO) complexes have been reported only very recently, the species concerned being [Pd(η^3-C_4H_7)($SnCl_3$)(CO)][9] and the anionic complexes [PdX_3(CO)]$^-$ (X = Cl or Br).[10] The molecular structures of the aqua and carbonyl complexes described in the present work, [2-(H_2O)-2-(PPh_3)-*closo*-2,1-$PdTeB_{10}H_9(PPh_3)$][BF_4] **2** and [2-(CO)-2-(PPh_3)-*closo*-2,1-$PdTeB_{10}H_9(PPh_3)$][BF_4] **3**, were determined using X-ray crystallography.

Results and Discussion

The reaction between equimolar amounts of Cs[*nido*-7-$TeB_{10}H_{11}$] and [$PdI_2(PPh_3)_2$] in refluxing toluene for 17 h affords [2-I-2-(PPh_3)-*closo*-2,1-$PdTeB_{10}H_9(PPh_3)$] **1** in excellent

† *Supplementary data available:* see Instructions for Authors, *J. Chem. Soc., Dalton Trans.*, 1993, Issue 1, pp. xxiii–xxviii.

$$[7\text{-TeB}_{10}H_{11}]^- + [PdI_2(PPh_3)_2] \xrightarrow{\text{toluene}} \underset{\mathbf{1}}{[2\text{-I-2-(PPh}_3)\text{-2,1-PdTeB}_{10}H_9(PPh_3)]} + I^- + H_2 \quad (1)$$

yield (95.4%), reaction (1).[6] When **1** was allowed to react with $Ag[BF_4]$ in toluene for 30 min, with the products being separated and purified under aerobic conditions, the green aquapalladium complex $[2\text{-}(H_2O)\text{-}2\text{-}(PPh_3)$-*closo*-2,1-PdTe-$B_{10}H_9(PPh_3)][BF_4]$ **2** was isolated in excellent yield (94.3%), reaction (2).

$$\mathbf{1} + Ag[BF_4] \xrightarrow{\text{toluene-water}} \underset{\mathbf{2}}{[2\text{-}(H_2O)\text{-}2\text{-}(PPh_3)\text{-}2,1\text{-PdTeB}_{10}H_9(PPh_3)][BF_4]} + AgI \quad (2)$$

Initial characterisation of compound **2** by infrared and ^1H, ^{11}B and ^{31}P NMR spectroscopies suggested the presence of the aqua ligand, the tetrafluoroborate ion, the B–PPh$_3$ unit and the *closo* nature of the $PdTeB_{10}$ cage. Absorptions were observed in the infrared regions associated with O–H (at 3395 and 1605 cm^{-1}), B–H (at 2540 cm^{-1}) and B–F (1094 cm^{-1}) bonds as well as with the PPh$_3$ ligand. The 128 MHz ^{11}B-{^1H} and 400 MHz ^1H-{^{11}B} NMR spectra showed nine BH units which were correlated using ^1H-{^{11}B(selective)} experiments, Table 1. This Table also contains data from $[2\text{-Cl-2-(PPh}_3)$-*closo*-2,1-$PdTeB_{10}H_9(PPh_3)]$ **13** and $[2,2\text{-}(PPh_3)_2$-*closo*-2,1-PdTe-$B_{10}H_{10}]$ **14**.[1] The assignments given in Table 1 were based on similarities in chemical shifts and peak widths with data from $[2\text{-Cl-2-(PPh}_3)$-*closo*-2,1-$PdTeB_{10}H_9(PPh_3)]$ and related compounds.[1] Additional data from ^{31}P NMR spectroscopy confirmed the presence of a B–PPh$_3$ unit with $^1J(^{31}P–^{11}B)$ 133 Hz, Table 1. The ^1H, ^{11}B and ^{31}P chemical shifts and coupling constant parameters for the cationic cluster **2** and neutral clusters **13** and **14** are remarkably similar which strongly suggests closely similar gross electronic structures of the *closo* cages. As well as the single BP and the nine BH signals observed in the ^{11}B NMR spectrum of **2**, there was a very sharp signal of unit relative intensity due to the $[BF_4]^-$ anion at δ −1.1.

Owing to the availability of good-quality crystals of compound **2** which were suitable for X-ray analysis, and the notable lack of structural data on aquapalladium complexes, we decided to determine the solid-state molecular structure of **2**. A view of the 7-PPh$_3$ enantiomer of the cation is shown in Fig. 1 and Table 2 lists selected interatomic distances and angles in this cation. Overall, the cage structure is typical of *closo* twelve-atom MXB_{10} clusters.[1,11–13] A notable feature of the cage geometry is the almost symmetrical bonding of the palladium atom to the TeB_4 face of the TeB_{10} ligand. The Pd–B(7) distance is 2.289(6) Å, slightly shorter than Pd–B(3) of 2.299(6) Å and, likewise, Pd–B(11) [2.192(6) Å] is slightly shorter than Pd–B(6) [2.197(6) Å]. The Pd–Te distance is 2.6958(6) Å. The ranges of the cage interatomic Te–B and B–B distances are 2.287(6)–2.403(6) Å and 1.737(9)–1.924(10) Å respectively. These are similar to those observed in other $PdTeB_{10}$ clusters.[1] The *exo*-cage B–P bond length is 1.950(6) Å.

The Pd–OH$_2$ bond length of 2.208(4) Å in compound **2** is essentially the same as that of 2.20(1) Å previously reported in $[Pd(bquin)(dmp)(H_2O)][ClO_4]$ **11**.[7] These bonds are longer than that of 2.132(3) Å observed in $[PdL'(H_2O)(ONO_2)]$-$[ClO_4]\cdot H_2O$ **12**.[8] The Pd–OH$_2$ distance in **2** may also be compared to the Pd–OH distance of 1.966(3) Å in $[Pd(terpy)$-$(OH)][ClO_4]\cdot H_2O$ (terpy = 2,2′:6′,2″-terpyridine),[14] or the Pd–O$_2$CMe distance of 2.121(3) Å in the neutral, monodentate acetate-containing cluster, $[2\text{-}(O_2CMe)\text{-}2\text{-}(PPh_3)$-*closo*-2,1-$PdTeB_{10}H_9(PPh_3)]$ **15**, which is closely related to **2**.[6]

The water molecule in compound **2** is easily displaced by other Lewis bases such as CO, isocyanides, acetonitrile, amines, phosphines, ethers and thioethers to afford the cationic complexes **3**–**10**, Scheme 1. At room temperature, compounds **2** and

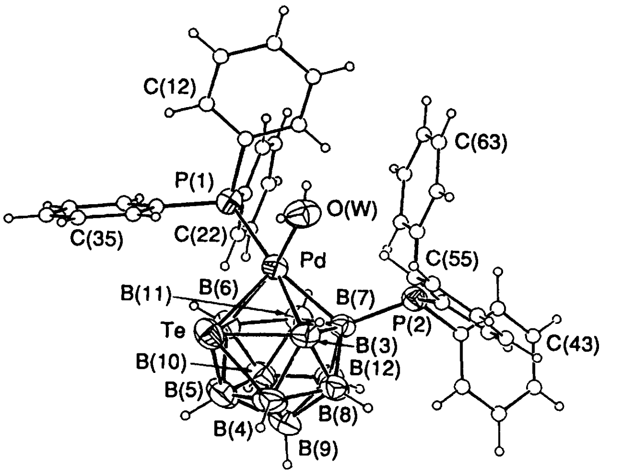

Fig. 1 General view of the cation of the 7-PPh$_3$ enantiomer of the complex $[2\text{-}(H_2O)\text{-}2\text{-}(PPh_3)$-*closo*-2,1-$PdTeB_{10}H_9(PPh_3)][BF_4]$ **2** showing the numbering scheme

$$\mathbf{2} \xrightarrow{(i)-(iii)} \underset{\mathbf{3-9}}{[2\text{-L-2-(PPh}_3)\text{-}closo\text{-2,1-PdTeB}_{10}H_9(PPh_3)][BF_4]}$$

$$\mathbf{2} \xrightarrow{(iv)} \underset{\mathbf{10}}{[2,2\text{-(PMe}_2Ph)\text{-}closo\text{-2,1-PdTeB}_{10}H_9(PPh_3)][BF_4]}$$

Scheme 1 (*i*) L = CO, toluene, 5 min, yield 39% (*ii*) L = Bu^{t}NC, $C_6H_{11}NC$, MeCH(Ph)NH$_2$ or C_4H_8S, **2**:L ratio 1:1, CH$_2$Cl$_2$, 30 min, yields 85, 93, 42 and 87% respectively; (*iii*) L = MeCN or thf, **2**:L ratio 1:1000, CH$_2$Cl$_2$, 30 min, yields 90 and 93% respectively; compound numbering sequence L = CO **3**, Bu^{t}NC **4**, $C_6H_{11}NC$ **5**, MeCN **6**, MeCH(Ph)NH$_2$ **7**, tetrahydrothiophene **8** or thf **9**; (*iv*) L = PMe$_2$Ph, **2**:L ratio 1:11, CH$_2$Cl$_2$, 30 min, yield 75%

3–**10** are generally air- and water-stable as well as being stable in polar and non-polar solvents. The crimson carbonyl compound **3**, which is the least stable of the compounds discussed here, is the exception to this generalisation. It evolves CO very slowly at room temperature. All compounds **3**–**10** were characterised by elemental analysis together with infrared and ^{11}B-{^1H} NMR spectroscopies. The infrared spectra showed strong absorption-band maxima corresponding to BH vibrations in the region 2570–2510 cm^{-1} and to BF vibrations in the region 1100–1000 cm^{-1} which were centred around *ca.* 1070 cm^{-1}. Also, there were specific absorption bands associated with each ligand L (see Experimental section for details).

Measured ^{11}B and ^{11}B-{^1H} NMR data (CD$_2$Cl$_2$ at 294–298 K) showed eleven boron atoms present in all compounds **3**–**10** with some overlapping of peaks even in spectra recorded at the ^{11}B frequency of 128 MHz. The B–H/B–X signals were in the δ(^{11}B) range from *ca.* +19 to *ca.* −21 and grouped with an intensity ratio of 1:(1:1):(1:1):1:1:(1:1):1:1. In each ^{11}B-{^1H} spectrum there was one signal of unit intensity between δ +9 and +11.5 coupled to ^{31}P, [$^1J(^{31}P–^{11}B)$ 130 ± 10 Hz] and one signal of unit intensity due to $[BF_4]^-$ at δ −1.2 ± 0.3. This latter signal is notably very much sharper than the others. The ^{11}B-{^1H}, ^1H-{^{11}B} and ^{31}P NMR data for the compounds with L = Bu^{t}NC **4**, tht **8** and $[2,2\text{-}(PMe_2Ph)_2$-*closo*-2,1-$PdTeB_{10}H_9(PPh_3)][BF_4]$ **10** are listed in Table 1. The assignments were made in the same way as for **2**. The NMR spectra are remarkably similar (Fig. 2) and confirm that all the compounds **2**–**10** are mutually analogous.

The palladium carbonyl complex, $[2\text{-(CO)-2-(PPh}_3)$-*closo*-2,1-$PdTeB_{10}H_9(PPh_3)][BF_4]$ **3** afforded crystals from toluene–

Table 1 Measured NMR parameters for $[2\text{-L-2-(PPh}_3)\text{-}closo\text{-2,1-PdTeB}_{10}\text{H}_9\text{(PPh}_3)][\text{BF}_4]$ (L = H_2O **2**, Bu^{t}NC **4** or C_4H_8S **8**, $[2,2\text{-(PMe}_2\text{Ph)}_2\text{-}closo\text{-2,1-PdTeB}_{10}\text{H}_9\text{(PPh}_3)][\text{BF}_4]$ **10**, $[2\text{-Cl-2-(PPh}_3)\text{-}closo\text{-2,1-PdTeB}_{10}\text{H}_9\text{(PPh}_3)]$ **13** and $[2,2\text{-(PPh}_3)_2\text{-}closo\text{-2,1-PdTeB}_{10}\text{H}_{10}]$ **14** in CD_2Cl_2 solution at 294–297 K

	2^b		**4**^{c}		**8**^{d}		**10**^{e}		**13**^{f}		**14**	
Assignment^a	$\delta(^{11}B)^g$	$\delta(^1H)^h$	$\delta(^{11}B)^g$	$\delta(^1H)^h$	$\delta(^{11}B)^g$	$\delta(^1H)^h$	$\delta(^{11}B)^g$	$\delta(^1H)^h$	$\delta(^{11}B)^g$	$\delta(^1H)^h$	$\delta(^{11}B)^g$	$\delta(^1H)^h$
(12)	+18.8	+5.42	+19.2	+5.45	+18.6	+5.45	+19.0	+5.32	+18.0	+4.96	+23.2	+5.74
(7,11)	*ca.* +10.8	+3.74	+13.0	+3.85	*ca.* +12.0	+3.39	+10.8	+4.07	+10.5	P sub.	+16.8	+4.90
	+10.9	P sub.	+9.7	P sub.	+11.4	P sub.	+7.2	P sub.	+9.2	+3.40		
(9)	+6.0	+5.01	+8.1	+5.13	+7.7	+5.00	+8.0	+5.05	+3.5	+4.73	+9.4	+4.96
(3,6)^i	+4.5	+2.61	*ca.* +6.5	+2.79	*ca.* +9.0	+3.27	+6.5	+2.90	+6.0	+2.79	+3.4^i	+1.96
	ca. −1.5	+2.33	−4.8	+2.33	−5.1	+1.78	−5.4	+1.82	−5.0	+2.01		
(4,5)^i	*ca.* −9.4	+2.80	*ca.* −9.0	+2.98	*ca.* −10.0	+2.84	−8.7	+3.16	−10.7	+3.18	−11.0	+2.76
	−12.3	+3.12	*ca.* −11.0	+3.25	*ca.* −10.0	+3.36	−10.3	+3.42	−10.0	+2.79		
(8,10)	−19.1	+1.83	−16.1	+2.30	−16.4	+2.16	−17.1	+2.33	−19.6	+1.70	−18.4	+1.58
	−20.7	+1.64	−18.3	+1.88	−18.4	+1.73	−19.1	+1.88	−21.9	+1.47		

^{a} On the basis of relative intensities together with shielding and linewidth parallels with previously reported analogues (see ref. 6 and Fig. 2). ^{b} $\delta(^{31}P)$ +30.5 (Pd) and *ca.* +7.1 (B) [$^1J(^{31}P\text{–}^{11}B)$ 133 ± 10 Hz]; $\delta(^1H)$ +2.62 (br, H_2O); $\delta(^{11}B)$ −1.1 (BF_4^-). ^{c} $\delta(^{31}P)$ +28.5 (Pd) and +10.8 (B) [$^1J(^{31}P\text{–}^{11}B)$ 128 ± 10 Hz]; $\delta(^1H)$ +1.01 (Bu^{t}NC); $\delta(^{11}B)$ −0.9 (BF_4^-). ^{d} $\delta(^{31}P)$ +34.7 (Pd) and *ca.* +9.4 (B) [$^1J(^{31}P\text{–}^{11}B)$ 133 ± 10 Hz]. ^{e} $\delta(^{31}P)_A$ +10.2 (B) [$^1J(^{31}P\text{–}^{11}B)$ 126 ± 10], $\delta(^{31}P)_B$ [d, $^2J(^{31}P_B\text{–}^{31}P_C)$ 46.5 Hz], $\delta(^{31}P)_C$ −7.5 (d of d, Pd) [$^2J(^{31}P_B\text{–}^{31}P_C)$ 46.5 and $^3J(^{31}P_A\text{–}^{31}P_C)$ 7.0 Hz]; $\delta(^1H)$ +7.8–+7.0 (PhP), +1.74 [d, MeP$_B$, $^2J(^{31}P_B\text{–}^1H)$ 10.0, 3 H], +1.72 [d, MeP$_B$, $^2J(^{31}P_B\text{–}^1H)$ 10.0, 3H], +0.92 [d, MeP$_C$, $^2J(^{31}P_C\text{–}^1H)$ 9.6, 3 H], +0.84 [d, MeP$_C$, $^2J(^{31}P_C\text{–}^1H)$ 9.6 Hz, 3 H]; $\delta(^1H)$ of PMe groups related to $\delta(^{31}P)$ by $^1H\text{–}\{^{31}P\}$ experiments; $\delta(^{11}B)$ −1.0 (BF_4^-). ^{f} $\delta(^{31}P)$ +31.2 (Pd) and +11.4 (B) [$^1J(^{31}P\text{–}^{11}B)$ 135 Hz].[6] ^{g} $\delta(^{11}B)$ ±0.5 ppm to high frequency (low field) of $BF_3\cdot OEt_2$. ^{h} ±0.05 Hz to high frequency (low field) of $SiMe_4$; ^1H resonances were related to directly bound B positions by $^1H\text{–}\{^{11}B\text{(selective)}\}$ spectroscopy. ^{i} The ^{11}B resonance lines are substantially broader (*i.e.* 300–400 Hz) than the other lines (< *ca.* 200 Hz).

Table 2 Selected interatomic distances (Å) and angles (°) in the cation $[2\text{-(H}_2\text{O)-2,7-(PPh}_3)_2\text{-}closo\text{-2,1-PdTeB}_{10}\text{H}_9]^+$ of compound **2**

Pd–Te	2.6958(6)	B(6)–B(10)	1.737(9)	Te–B(6)	2.403(6)	B(10)–B(12)	1.768(9)
Pd–P(1)	2.3544(14)	B(6)–B(11)	1.913(8)	B(3)–B(4)	1.922(9)	B(11)–B(12)	1.772(9)
Pd–O(W)	2.208(4)	B(7)–B(8)	1.763(8)	B(3)–B(7)	1.817(8)	P(2)–B(7)	1.950(6)
Pd–B(3)	2.299(6)	B(7)–B(11)	1.772(8)	B(3)–B(8)	1.764(9)	P(1)–C(11)	1.822(5)
Pd–B(6)	2.197(6)	B(7)–B(12)	1.763(8)	B(4)–B(5)	1.882(11)	P(1)–C(21)	1.830(5)
Pd–B(7)	2.289(6)	B(8)–B(9)	1.808(9)	B(4)–B(8)	1.763(10)	P(1)–C(31)	1.823(5)
Pd–B(11)	2.192(6)	B(8)–B(12)	1.794(9)	B(4)–B(9)	1.766(11)	P(2)–C(41)	1.808(5)
Te–B(3)	2.386(6)	B(9)–B(10)	1.797(10)	B(5)–B(6)	1.924(10)	P(2)–C(51)	1.811(5)
Te–B(4)	2.288(7)	B(9)–B(12)	1.764(8)	B(5)–B(9)	1.739(11)	P(2)–C(61)	1.808(5)
Te–B(5)	2.287(6)	B(10)–B(11)	1.788(8)	B(5)–B(10)	1.761(10)		
P(1)–Pd–O(W)	94.22(11)	B(3)–B(7)–B(8)	59.0(3)	B(4)–B(3)–B(8)	56.9(3)	B(10)–B(11)–B(12)	59.6(4)
Te–Pd–B(3)	56.41(16)	B(8)–B(7)–B(12)	61.2(3)	B(7)–B(3)–B(8)	59.0(3)	B(7)–B(12)–B(8)	59.4(3)
Te–Pd–B(6)	57.75(17)	B(11)–B(7)–B(12)	60.2(3)	Te–B(4)–B(5)	65.7(3)	Pd–P(1)–C(11)	109.26(16)
B(3)–Pd–B(7)	46.65(21)	B(4)–B(8)–B(9)	59.3(4)	B(3)–B(4)–B(8)	57.0(3)	Pd–P(1)–C(21)	118.12(16)
B(6)–Pd–B(11)	51.67(23)	B(9)–B(8)–B(12)	58.6(4)	B(5)–B(4)–B(9)	56.8(4)	Pd–P(1)–C(31)	113.19(17)
B(7)–Pd–B(11)	46.53(21)	B(5)–B(9)–B(10)	59.7(4)	B(8)–B(4)–B(9)	61.4(4)	B(7)–P(2)–C(41)	113.09(24)
Pd–Te–B(3)	53.37(14)	B(8)–B(9)–B(12)	60.3(3)	Te–B(5)–B(6)	69.0(3)	B(7)–P(2)–C(51)	111.57(23)
Pd–Te–B(6)	50.65(14)	B(10)–B(9)–B(12)	59.5(4)	B(4)–B(5)–B(9)	58.2(4)	B(7)–P(2)–C(61)	111.29(23)
B(3)–Te–B(4)	48.51(23)	B(6)–B(10)–B(11)	65.7(3)	B(6)–B(5)–B(10)	56.0(4)	Pd–B(7)–P(2)	116.0(3)
B(4)–Te–B(5)	48.6(3)	B(9)–B(10)–B(12)	59.3(4)	Te–B(6)–B(11)	62.7(3)	B(3)–B(7)–P(2)	118.0(3)
B(5)–Te–B(6)	48.4(3)	B(11)–B(10)–B(12)	59.8(3)	B(5)–B(6)–B(10)	57.2(4)	B(8)–B(7)–P(2)	114.6(4)
Te–B(3)–B(4)	63.1(3)	Pd–B(11)–B(6)	64.3(3)	B(10)–B(6)–B(11)	58.5(3)	B(11)–B(7)–P(2)	125.1(4)
Pd–B(3)–B(7)	66.4(3)	B(7)–B(11)–B(12)	59.7(3)	Pd–B(7)–B(11)	63.9(3)	B(12)–B(7)–P(2)	119.3(4)

light petroleum solution which were suitable for X-ray analysis. Table 3 gives selected interatomic distances and angles in the 11-PPh_3 enantiomer of the cation of **3** and the molecular structure of this cation is shown in Fig. 3. Compound **3** is the first cationic monopalladium carbonyl complex to be structurally characterised. Previously, the neutral complex $[Pd(\eta^3\text{-}C_4H_7)(SnCl_3)(CO)]$[9] and the anionic species $[PdX_3(CO)]^-$ (X = Cl or Br)[10] had been reported. The palladium–carbon distance in **3** is 2.003(9) Å which is longer than the distances in either the allyl complex, 1.947(11) Å, or the anions, 1.87(1) and 1.87(3) Å for X = Cl and Br respectively. Both the neutral and anionic complexes are unstable under aerobic conditions.[9,10] It is not clear why the relatively weak Pd–CO bond in **3** appears to be more stable to aerial oxidation and thermal decomposition than the Pd–CO bonds in the neutral and anionic complexes. It is possible that the combined bulk of the telluraborane cage and the triphenylphosphine ligands is sufficient to inhibit the oxidation reaction effectively, but it is difficult to see why the thermal decomposition reaction is also inhibited in **3** compared with the other palladium carbonyl complexes.

The integrity of the twelve-vertex $PdTeB_{10}$ cage which was present in the original reagent, $[2\text{-I-2-(PPh}_3)\text{-}closo\text{-2,1-PdTeB}_{10}\text{H}_9\text{(PPh}_3)]$ **1**, is retained in the cation of **3**, Fig. 2. In general, the cage interatomic distances in **2** and **3** are remarkably similar and close to those in the neutral species $[2\text{-(O}_2\text{CMe)-2-(PPh}_3)\text{-}closo\text{-2,1-PdTeB}_{10}\text{H}_9\text{(PPh}_3)]$ **15** and $[2,2\text{-(PMe}_2\text{Ph)}_2\text{-}closo\text{-2,1-PdTeB}_{10}\text{H}_{10}]$ **16**.[1] The major differences between these compounds are that: (*i*) the Pd–Te distance in **2**, 2.6958(6) Å, is significantly longer than in **3** or **15** which are the same within experimental error at 2.6897(9) and 2.6903(4) Å respectively, whereas that in **16** is significantly shorter at 2.6833(2) Å; (*ii*) the ranges of B–B distances in **2** and **3** of 1.737(9)–1.924(10) and 1.744(15)–1.929(14) Å are very similar

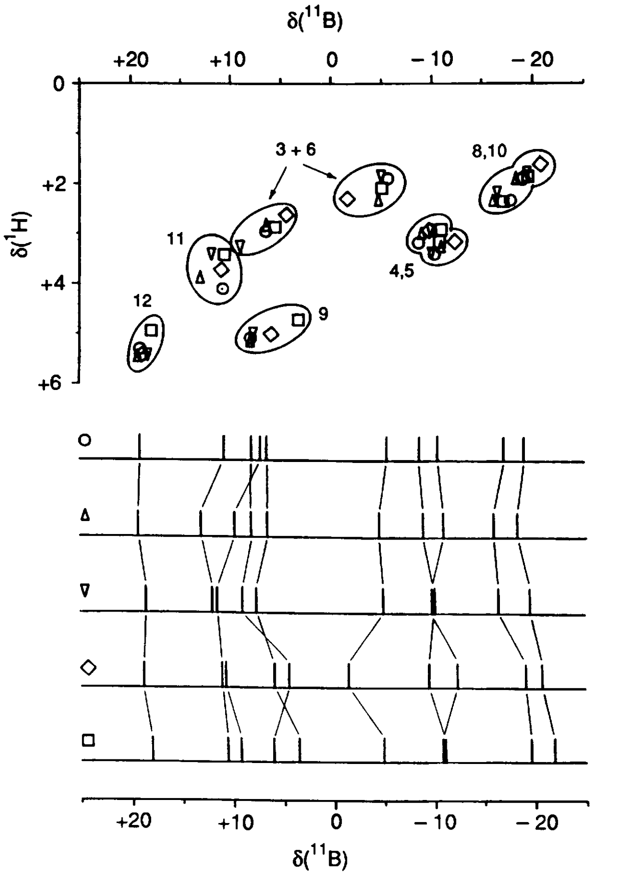

Fig. 2 Cluster ^{11}B and ^{1}H NMR data for the neutral compound **13** (□), for the tetrafluoroborate salts of the cationic species $[2\text{-L-}2\text{-}(PPh_3)\text{-}closo\text{-}2,1\text{-}PdTeB_{10}H_9(PPh_3)\text{-}7]^+$ where L = H_2O (complex **2**, ◇), C_4H_8S (**8**, ▽) or Bu^{t}NC (**4**, △), and for complex **10** (○). The top diagram is a plot of δ(^{1}H) *versus* δ(^{11}B) for the individual BH cluster units, and the bottom diagrams are stick representations of the ^{11}B chemical shifts, with lines drawn to show the equivalent positions for the various species

and slightly smaller than the ranges in **15** and **16** which are 1.753(7)–1.978(7) and 1.733(5)–1.940(4) Å respectively; (*iii*) the Pd–B distances which are '*cis*' to the phosphine in **2**, 2.192(6) and 2.197(6) Å respectively, and **3**, 2.195(10) and 2.282(10) Å respectively, are shorter than those which are '*trans*' to the phosphine, 2.289(6) and 2.299(6) Å in **2**, and 2.290(9) and 2.307(9) Å in **3** respectively; this is also the case in **15**; (*iv*) the B–P distances in **2**, **3** and **15** are the same within experimental error, at 1.950(6), 1.941(9) and 1.942(4) Å respectively; (*v*) the Pd–P distance in **3**, 2.3673(21) Å is significantly longer than those in **2** and **15** which are essentially the same at 2.3544(14) and 2.355(1) Å respectively.

Comments on the Preparation of Cationic Metallaheteroboranes.—The route to the synthesis of the metallaheteroborane cations described in this paper was facilitated by the initial high-yield synthesis of a metal halide-containing complex *i.e.* $[2\text{-I-}2\text{-}(PPh_3)\text{-}closo\text{-}2,1\text{-}PdTeB_{10}H_9(PPh_3)]$ **1**.[1] In Part 11 of this series[1] we demonstrated that **1** was produced as the sole product of the reaction between *trans*-$[PdI_2(PPh_3)_2]$ and $[nido\text{-}7\text{-}TeB_{10}H_{11}]^-$ when the reaction was carried out in refluxing toluene solution, reaction (1). Under those conditions the palladium reagent is thought to retain the *trans* stereochemistry. By contrast, under other conditions, for example if the solvent was thf, the palladium complex, say $[PdCl_2(PPh_3)_2]$, and the reaction temperature ambient, the palladium reagent exists as a mixture of *cis* and *trans* isomers. In this case, the *cis* isomer is thought to react faster than the *trans* isomer affording $[2,2\text{-}(PPh_3)_2\text{-}closo\text{-}2,1\text{-}PdTeB_{10}H_{10}]$ **14** as the only isolable palladatelluraborane.[1]

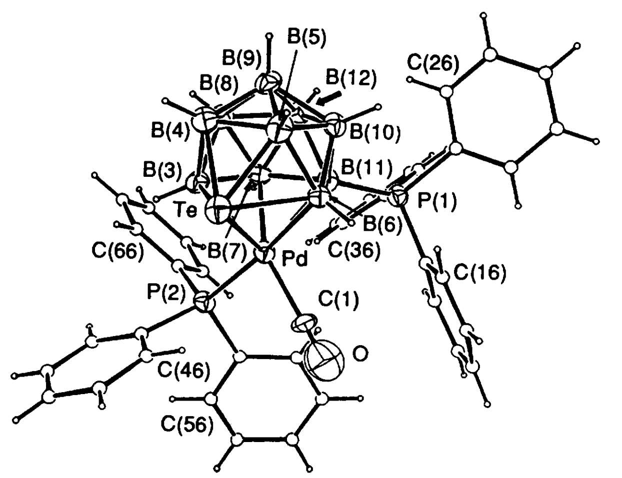

Fig. 3 General view of the cation of the 11-PPh_3 enantiomer of the complex $[2\text{-}(CO)\text{-}2\text{-}(PPh_3)\text{-}closo\text{-}2,1\text{-}PdTeB_{10}H_9(PPh_3)][BF_4]$ **3** showing the numbering scheme

We anticipate that the subsequent step which converts compound **1** into **2** may be of general use in the synthesis of cationic metallaheteroboranes, although it is possible that a suitable ligand may have to be added immediately after the addition of the silver salt to stabilise the cationic products, reaction (3). Work is currently in hand which aims to use the

$$[\text{cluster (M–X)}] \xrightarrow[(ii)\ +\ :L]{(i)\ +\ Ag^+\ (-X^-)} [\text{cluster (M–L)}]^+ \quad (3)$$

principle embodied in reaction (3) to synthesise air-stable metalla-borane and -carborane cations and to extend the number of metallaheteroborane cations known.

Experimental

General.—All preparative experiments and recrystallisations were carried out in an inert atmosphere. The compound $[2\text{-I-}2\text{-}(PPh_3)\text{-}closo\text{-}2,1\text{-}PdTeB_{10}H_9(PPh_3)]$ **1** was prepared as previously described.[1] Infrared spectra were recorded as KBr discs on Perkin Elmer 682 or Mattson Polaris FTIR spectrometers, NMR spectra with the techniques described in earlier parts of this series.[1,11–13] Data in Table 1 were obtained with a Bruker AM400 instrument and remaining data were obtained with a JEOL 270GSX spectrometer. Chemical shifts (δ) are quoted to low frequency (high field) of Ξ 100 MHz for ^{1}H, Ξ 32.083 971 MHz for ^{11}B (nominally $F_3B{\cdot}OEt_2$ in CD_2Cl_2) and Ξ 40.480 730 MHz for ^{31}P (nominally 85% H_3PO_4); peak shapes are designated as vsh (very sharp), sh (sharp), br (broad) or vbr (very broad).

Reaction of $[2\text{-I-}2\text{-}(PPh_3)\text{-}closo\text{-}2,1\text{-}PdTeB_{10}H_9(PPh_3)]$ **1** *with* $Ag[BF_4]$.—A suspension of $Ag[BF_4]$ (0.081 g, 0.414 mmol) in toluene (20 cm^3) was added to a solution of $[2\text{-I-}2\text{-}(PPh_3)\text{-}closo\text{-}2,1\text{-}PdTeB_{10}H_9(PPh_3)]$ **1** (0.415 g, 0.414 mmol) in toluene (100 cm^3). The solution, which initially was dark green, immediately lightened and a yellow precipitate formed. After stirring the mixture at room temperature for 30 min, it was filtered. The solution was collected and the solvent removed under reduced pressure (rotary evaporator, 35 °C). Recrystallisation from CH_2Cl_2–heptane (1:1, 30 cm^3) afforded green crystalline blocks of $[2\text{-}(H_2O)\text{-}2\text{-}(PPh_3)\text{-}closo\text{-}2,1\text{-}PdTeB_{10}H_9\text{-}(PPh_3)][BF_4]{\cdot}0.89CH_2Cl_2$, **2**·$0.89CH_2Cl_2$ (0.383 g, 94.3%) (Found: C, 41.60; H, 4.25. $C_{36}H_{41}B_{11}F_4OP_2PdTe{\cdot}0.89CH_2Cl_2$

Table 3 Selected interatomic distances (Å) and angles (°) in the cation $[2\text{-}(CO)\text{-}2,11\text{-}(PPh_3)_2\text{-}closo\text{-}2,1\text{-}PdTeB_{10}H_9]^+$ of compound **3**

Pd–Te	2.6897(9)	B(6)–B(10)	1.787(13)	Te–B(6)	2.389(9)	B(10)–B(12)	1.774(14)
Pd–P(2)	2.3673(21)	B(6)–B(11)	1.825(13)	B(3)–B(4)	1.915(14)	B(11)–B(12)	1.781(14)
Pd–C(1)	2.003(9)	B(7)–B(8)	1.791(14)	B(3)–B(7)	1.889(13)	P(1)–B(11)	1.941(9)
Pd–B(3)	2.282(10)	B(7)–B(11)	1.797(13)	B(3)–B(8)	1.744(15)	O–C(1)	1.019(15)
Pd–B(6)	2.307(9)	B(7)–B(12)	1.791(13)	B(4)–B(5)	1.876(16)	P(1)–C(11)	1.808(9)
Pd–B(7)	2.195(10)	B(8)–B(9)	1.828(14)	B(4)–B(8)	1.795(15)	P(1)–C(21)	1.816(8)
Pd–B(11)	2.290(9)	B(8)–B(12)	1.791(14)	B(4)–B(9)	1.756(15)	P(1)–C(31)	1.816(9)
Te–B(3)	2.338(11)	B(9)–B(10)	1.796(15)	B(5)–B(6)	1.929(14)	P(2)–C(41)	1.839(8)
Te–B(4)	2.285(12)	B(9)–B(12)	1.762(14)	B(5)–B(9)	1.788(16)	P(2)–C(51)	1.818(9)
Te–B(5)	2.262(11)	B(10)–B(11)	1.770(12)	B(5)–B(10)	1.797(14)	P(2)–C(61)	1.801(9)
P(2)–Pd–C(1)	92.5(3)	B(8)–B(7)–B(12)	60.0(5)	B(7)–B(3)–B(8)	58.9(5)	Pd–C(1)–O	177.0(1)
Te–Pd–B(3)	55.4(3)	B(11)–B(7)–B(12)	59.5(5)	Te–B(4)–B(5)	65.0(5)	Pd–P(2)–C(41)	114.1(3)
Te–Pd–B(6)	56.51(22)	B(4)–B(8)–B(9)	58.0(6)	B(3)–B(4)–B(8)	56.0(5)	Pd–P(2)–C(51)	112.0(3)
B(3)–Pd–B(7)	49.9(4)	B(9)–B(8)–B(12)	58.3(5)	B(5)–B(4)–B(9)	58.9(6)	Pd–P(2)–C(61)	117.4(3)
B(6)–Pd–B(11)	46.8(3)	B(5)–B(9)–B(10)	60.2(6)	B(8)–B(4)–B(9)	61.9(6)	B(11)–P(1)–C(11)	111.8(4)
B(7)–Pd–B(11)	47.2(3)	B(8)–B(9)–B(12)	59.8(6)	Te–B(5)–B(6)	69.0(4)	B(11)–P(1)–C(21)	114.8(4)
Pd–Te–B(3)	53.43(23)	B(10)–B(9)–B(12)	59.8(6)	B(4)–B(5)–B(9)	57.2(6)	B(11)–P(1)–C(31)	111.6(4)
Pd–Te–B(6)	53.64(21)	B(6)–B(10)–B(11)	61.7(5)	B(6)–B(5)–B(10)	57.2(5)	Pd–B(11)–P(1)	118.0(4)
B(3)–Te–B(4)	48.9(3)	B(9)–B(10)–B(12)	59.1(6)	B(9)–B(5)–B(10)	60.1(6)	B(6)–B(11)–P(1)	121.3(6)
B(4)–Te–B(5)	48.7(4)	B(11)–B(10)–B(12)	60.3(5)	Pd–B(6)–B(11)	66.1(4)	B(7)–B(11)–P(1)	125.0(5)
B(5)–Te–B(6)	48.9(3)	Pd–B(11)–B(6)	67.1(4)	B(5)–B(6)–B(10)	57.7(5)	B(10)–B(11)–P(1)	114.2(5)
Te–B(3)–B(4)	64.1(5)	B(7)–B(11)–B(12)	60.1(5)	B(10)–B(6)–B(11)	58.7(5)	B(12)–B(11)–P(1)	115.8(6)
Pd–B(3)–B(7)	62.7(4)	B(10)–B(11)–B(12)	60.0(5)	B(3)–B(7)–B(8)	56.5(5)		
B(4)–B(3)–B(8)	58.6(6)	B(7)–B(12)–B(8)	60.0(5)				

requires C, 41.95; H, 4.10%). IR: ν_{max} 3395m (br) (H_2O), 2540vs (BH), 1605w (br)(H_2O) and 1094vs (br) cm^{-1} (BF_4^-). NMR data in Table 1.

Reaction of $[2\text{-}(H_2O)\text{-}2\text{-}(PPh_3)\text{-}closo\text{-}2,1\text{-}PdTeB_{10}H_9(PPh_3)][BF_4]$ **2** *with Carbon Monoxide.*—Carbon monoxide was bubbled through a solution of compound **1** (0.053 g, 0.054 mmol) in toluene (30 cm^3). There was an immediate colour change from green to reddish pink. The flow of carbon monoxide was stopped after 5 min and the volume of the solution reduced to 6 cm^3 and over-layered with light petroleum (b.p. 100–120 °C) (10 cm^3). Red crystals of $[2\text{-}(CO)\text{-}2\text{-}(PPh_3)\text{-}closo\text{-}2,1\text{-}PdTeB_{10}H_9(PPh_3)][BF_4]\cdot C_6H_5Me$, **3**$\cdot C_6H_5Me$ (0.023 g, 39.3%) were obtained (Found: C, 46.65; H, 4.50. $C_{44}H_{47}B_{11}F_4OP_2PdTe$ requires C, 48.80; H, 4.40%). IR: ν_{max} 2540vs (BH), 2518s (sh)(BH), 2118vs (CO) and 1078vs (br) cm^{-1} (BF_4^-). $^{11}B\text{-}\{^1H\}$ NMR (CH_2Cl_2, 294–298 K); δ +19.6 (br, 1 B), +11.0 (br, 1 B), +10.4 [sh, 1 B, $J(^{11}B\text{-}^{31}P)$ *ca.* 130 ± 5 Hz], +5.9 (vbr, 2 B), −1.5 (vsh, 1 B), −10.1 (vbr, 1 B), −12.2 (vbr, 1 B), −15.0 (vbr, 1B), −18.6 (sh, 1 B) and −21.0 (sh, 1 B).

General Procedures for Reactions of Compound **2** *with Ligands* L.—*Procedure (a).* One equivalent of L in CH_2Cl_2 (5 cm^3) was added dropwise to a solution of compound **2** (*ca.* 0.1 mmol) in CH_2Cl_2 (20 cm^3). An immediate colour change occurred. The solution was stirred for 30 min, concentrated to *ca.* 5 cm^3 and layered with heptane (3 cm^3).

With Bu^{t}NC. Recrystallisation from CH_2Cl_2–toluene (3:2) gave red-pink crystals of $[2\text{-}(Bu^tNC)\text{-}2\text{-}(PPh_3)\text{-}closo\text{-}2,1\text{-}PdTeB_{10}H_9(PPh_3)][BF_4]\cdot C_6H_5Me$, **4**$\cdot C_6H_5Me$ (85.1%) (Found: C, 49.20; H, 4.95; N, 1.55. $C_{48}H_{56}B_{11}F_4NP_2PdTe$ requires C, 50.65; H, 4.95; N, 1.25%). IR: ν_{max} 2558vs (BH), 2208vs (CN) and 1058vs (br) cm^{-1} (BF_4^-). NMR data in Table 1.

With $C_6H_{11}NC$. Recrystallisation from CH_2Cl_2–heptane (3:1) gave reddish pink crystals of $[2\text{-}(C_6H_{11}NC)\text{-}2\text{-}(PPh_3)\text{-}closo\text{-}2,1\text{-}PdTeB_{10}H_9(PPh_3)][BF_4]\cdot C_6H_5Me$, **5**$\cdot 0.5CH_2Cl_2$ (93.0%) (Found: C, 46.50; H, 5.00; N, 0.85. $C_{43.5}H_{51}B_{11}ClF_4NP_2PdTe$ requires C, 46.90; H, 4.60; N, 1.25%). IR: ν_{max} 2560vs (BH), 2520vs (BH), 2215vs (CN) and 1055vs (br) cm^{-1} (BF_4^-). $^{11}B\text{-}\{^1H\}$ NMR (CH_2Cl_2, 294–298 K): δ +18.7 (br, 1 B), *ca.* + 13.0 (br, 1 B), +10.5 (br, 1 B), +9.7 [sh, 1 B, $J(^{11}B\text{-}^{31}P)$ *ca.* 132 ± 5 Hz], *ca.* +8.0 (vbr, 1 B), −1.3 (vsh, 1 B), *ca.* −6.0 (vbr, 1 B), −10.4 (vbr, 2 B), −16.5 (sh, 1 B) and −18.1 (sh, 1 B).

With (R)-(+)-1-*phenylethylamine*. Recrystallisation from CH_2Cl_2–heptane (3:1) gave purple needles of $[2\text{-}\{MeCH(Ph)NH_2\}\text{-}2\text{-}(PPh_3)\text{-}closo\text{-}2,1\text{-}PdTeB_{10}H_9(PPh_3)][BF_4]$ **7** (41.6%) (Found: C, 48.60; H, 4.65; N, 1.35. $C_{44}H_{50}B_{11}F_4NP_2PdTe$ requires C, 48.90; H, 4.65; N, 1.30%). IR: ν_{max} 3314m (NH), 3266m (NH), 2609m, 2524s, 2512vs (BH) and 1067s (br) cm^{-1} (BF_4^-). $^{11}B\text{-}\{^1H\}$ NMR (CH_2Cl_2, 294–298 K): δ +17.4 (br, 1 B), +9.3 [sh, 1 B, $J(^{11}B\text{-}^{31}P)$ *ca.* 132 ± 5 Hz], +8.5 (br, 1 B), *ca.* +7.1 (vbr, 2 B), −1.5 (vsh, 1 B), *ca.* −5.2 (vbr, 1 B), −12.1 (vbr, 2 B), *ca.* −19.9 (sh, 1 B) and −21.4 (sh, 1 B).

With tetrahydrothiophene. Recrystallisation from CH_2Cl_2–heptane (3:1) gave purple crystals of $[2\text{-}(C_4H_8S)\text{-}2\text{-}(PPh_3)\text{-}closo\text{-}2,1\text{-}PdTeB_{10}H_9(PPh_3)][BF_4]$ **8** (87.1%) (Found: C, 45.10; H, 4.65; S, 3.05. $C_{40}H_{47}B_{11}F_4P_2PdSTe$ requires C, 45.90; H, 4.55; S, 3.05%). IR: ν_{max} 2567 vs (BH) and 1062vs (br) cm^{-1} (BF_4^-). NMR data in Table 1.

Procedure (b). A large excess of L (5 cm^3 of MeCN or thf, or 11 equivalents of PMe_2Ph) was added dropwise to a solution of compound **2** (0.1 mmol) in CH_2Cl_2 (20 cm^3). An immediate colour change occurred. The solution was stirred for 30 min, concentrated to *ca.* 5 cm^3 and layered with heptane (3 cm^3).

With excess of MeCN. Recrystallisation from CH_2Cl_2–heptane (3:1) gave purple crystals of $[2\text{-}(MeCN)\text{-}2\text{-}(PPh_3)\text{-}closo\text{-}2,1\text{-}PdTeB_{10}H_9(PPh_3)][BF_4]$ **6** (89.9%) (Found: C, 44.95; H, 4.45; N, 1.85. $C_{38}H_{42}B_{11}F_4NP_2PdTe$ requires C, 45.50; H, 4.20; N, 1.40%). IR: ν_{max} 2558vs, 2548vs, 2511s (BH), 2336w (CN), 2289w (CN) and 1054vs (br) cm^{-1} (BF_4^-). $^{11}B\text{-}\{^1H\}$ NMR (CH_2Cl_2, 294–298 K): δ +18.1 (br, 1 B), +10.7 (br, 1 B), +9.9 [sh, 1 B, $J(^{11}B\text{-}^{31}P)$ = 132 ± 5 Hz], +7.0 (br, 2 B), −1.4 (vsh, 1 B), *ca.* −4.0 (vbr, 1 B), −11.3 (vbr, 2 B), −18.3 (sh, 1 B) and −19.7 (sh, 1 B).

With excess of thf. Recrystallisation from thf–heptane (3:2) gave blue crystals of $[2\text{-}(C_4H_8O)\text{-}2\text{-}(PPh_3)\text{-}closo\text{-}2,1\text{-}PdTeB_{10}H_9(PPh_3)][BF_4]\cdot C_4H_8O$, **9**$\cdot$thf (92.9%) (Found: C, 48.35; H, 5.25. $C_{44}H_{55}B_{11}F_4O_2P_2PdTe$ requires C, 47.75; H, 5.00%). IR: ν_{max} 2538vs (BH) and 1060vs (br) cm^{-1} (BF_4^-). $^{11}B\text{-}\{^1H\}$ NMR (CH_2Cl_2, 294–298 K): δ + 18.3 (br, 1 B), +10.4 [sh, 1 B, $J(^{11}B\text{-}^{31}P)$ *ca.* 128 ± 5 Hz], +9.7 (br, 1 B), +7.8 (br, 2 B), −1.5 (vsh, 1 B), *ca.* −1.6 (vbr, 1 B), −11.4 (vbr, 2 B), −19.9 (sh, 1 B) and −21.1 (sh, 1 B).

Table 4 Details of the data collection and refinement for compounds **2**·$0.89CH_2Cl_2$ and **3**·C_6H_5Me[a]

Molecule	**2**·$0.89CH_2Cl_2$	**3**·C_6H_5Me
Crystal size (mm)	0.23 × 0.26 × 0.40	0.36 × 0.33 × 0.15
Crystal colour and shape	Green block	Dark red block
Range of orienting reflections (°)	$7.5 < \theta < 17.5$	$7 < \theta < 18$
Range of *hkl* collected	*h* 0–17, *k* 0–19, *l* −25 to 25	*h* −18 to 18, *k* 0–13, *l* 0–39
Reflections collected	10 018	11 088
Independent reflections	9628	10 510
Observed reflections	5595 [$I > 3\sigma(I)$]	5439 [$I > 2.5\sigma(I)$]
Maximum and minimum transmission factors	0.98, 0.95	0.86, 0.72
Least-squares parameters	559	514
R	0.038	0.054
R'[b]	0.052	0.071
g	0.0012	0.001 25
Maximum shift/error	<0.07	<0.3
Maximum ρ/e Å^{-3}	0.7	1.45

[a] Details in common: ω–2θ scans; scan width 0.7 + 0.35 tanθ; 2θ limits 4–54°. [b] $R' = \{\Sigma[w(F_o - F_c)^2]/\Sigma(wF_o^2)\}^{\frac{1}{2}}$ where $w^{-1} = \sigma^2(F_o) + gF_o^2$.

Table 5 Positional parameters and their estimated standard deviations for compound **2**·0.89 CH_2Cl_2

Atom	*x*	*y*	*z*	Atom	*x*	*y*	*z*	Site occupancy
Te(1)	0.229 87(3)	0.617 25(3)	0.997 59(2)	C(53)	0.045 0(5)	0.539 7(4)	0.643 0(3)	
Pd	0.238 33(3)	0.749 16(2)	0.912 64(2)	C(54)	0.129 8(6)	0.498 7(4)	0.655 8(3)	
P(1)	0.339 27(9)	0.860 60(8)	0.953 46(6)	C(55)	0.201 0(5)	0.534 8(5)	0.697 2(3)	
P(2)	0.075 37(9)	0.747 14(8)	0.765 93(6)	C(56)	0.185 8(4)	0.611 4(4)	0.728 4(3)	
O(W)	0.338 4(3)	0.702 2(3)	0.842 5(2)	C(61)	0.154 3(4)	0.831 7(3)	0.743 7(2)	
C(11)	0.440 0(4)	0.868 9(3)	0.902 9(3)	C(62)	0.220 5(4)	0.822 0(4)	0.697 3(3)	
C(12)	0.535 0(4)	0.863 6(4)	0.928 0(3)	C(63)	0.276 7(5)	0.890 4(5)	0.681 6(3)	
C(13)	0.607 7(4)	0.868 1(4)	0.887 1(4)	C(64)	0.264 8(6)	0.968 0(5)	0.709 3(4)	
C(14)	0.586 8(5)	0.878 9(4)	0.820 2(4)	C(65)	0.198 1(6)	0.980 6(4)	0.755 7(4)	
C(15)	0.493 7(5)	0.886 0(4)	0.793 9(3)	C(66)	0.144 3(5)	0.911 6(4)	0.772 8(3)	
C(16)	0.420 6(4)	0.879 5(4)	0.834 9(3)	B(3)	0.151 5(4)	0.626 9(4)	0.888 8(3)	
C(21)	0.290 1(4)	0.968 9(3)	0.954 4(2)	B(4)	0.078 3(5)	0.582 0(4)	0.956 9(4)	
C(22)	0.210 1(4)	0.985 0(3)	0.988 4(2)	B(5)	0.084 4(6)	0.663 0(5)	1.025 8(3)	
C(23)	0.170 2(4)	1.066 2(4)	0.987 8(3)	B(6)	0.162 1(5)	0.757 9(4)	1.002 7(3)	
C(24)	0.210 4(5)	1.131 6(4)	0.953 3(3)	B(7)	0.090 1(4)	0.724 2(3)	0.860 8(3)	
C(25)	0.290 5(5)	1.116 7(4)	0.920 8(3)	B(8)	0.026 1(5)	0.634 6(4)	0.885 9(3)	
C(26)	0.331 3(4)	1.036 2(4)	0.921 5(3)	B(9)	−0.012 7(5)	0.657 5(5)	0.966 9(3)	
C(31)	0.394 2(3)	0.840 5(3)	1.036 7(2)	B(10)	0.038 4(5)	0.759 2(4)	0.991 1(3)	
C(32)	0.435 3(4)	0.761 8(3)	1.050 4(3)	B(11)	0.096 8(4)	0.803 2(4)	0.923 8(3)	
C(33)	0.478 8(5)	0.742 9(4)	1.112 5(3)	B(12)	−0.007 6(4)	0.740 6(4)	0.908 5(3)	
C(34)	0.478 7(5)	0.803 6(5)	1.161 9(3)	F(1)	0.419 8(4)	0.566 2(4)	0.914 5(4)	
C(35)	0.437 9(5)	0.882 0(4)	1.149 4(3)	F(2)	0.520 0(5)	0.467 5(3)	0.887 3(4)	
C(36)	0.395 6(4)	0.901 0(4)	1.086 6(3)	F(3)	0.388 5(6)	0.483 9(8)	0.830 0(4)	
C(41)	−0.043 8(4)	0.781 0(3)	0.737 0(3)	F(4)	0.494 7(10)	0.571 6(8)	0.815 8(6)	0.6
C(42)	−0.058 8(5)	0.849 1(4)	0.692 2(3)	F(5)	0.365 4(11)	0.434 0(11)	0.928 7(9)	0.4
C(43)	−0.150 8(6)	0.869 8(5)	0.668 8(4)	B(1)	0.456 4(13)	0.515 9(12)	0.861 2(10)	0.6
C(44)	−0.226 8(5)	0.823 9(5)	0.687 0(4)	B(2)	0.411 1(25)	0.493 8(26)	0.902 8(17)	0.4
C(45)	−0.211 9(4)	0.756 7(5)	0.730 8(3)	Cl(1)	0.267 6(3)	0.337 5(4)	1.098 1(3)	0.89
C(46)	−0.122 2(4)	0.736 0(4)	0.755 7(3)	Cl(2)	0.313 3(6)	0.357 6(6)	0.980 3(3)	0.53
C(51)	0.098 2(4)	0.652 6(3)	0.718 2(2)	Cl(3)	0.420 6(5)	0.347 0(4)	1.162 8(3)	0.36
C(52)	0.028 0(4)	0.616 9(4)	0.673 7(3)	C(S1)	0.356 0(12)	0.373 2(9)	1.068 0(9)	0.89

The site occupancy is 1.0 unless otherwise specified.

With excess of PMe_2Ph. Recrystallisation from CH_2Cl_2–heptane (3:2) gave red crystals of [2,2-$(PMe_2Ph)_2$-*closo*-2,1-$PdTeB_{10}H_9(PPh_3)$][BF_4]·$0.5CH_2Cl_2$, **10**·$0.5CH_2Cl_2$ (75.0%) (Found: C, 40.90; H, 4.75. $C_{34.5}H_{47}B_{11}ClF_4P_3PdTe$ requires C, 40.65; H, 4.70%). IR: ν_{max} 2509m, 2557vs, 2552vs, 2537vs, 2523vs (BH) and 1063vs cm^{-1} (BF_4^-). NMR data in Table 1.

Structure Determination of Compounds **2**·$0.89CH_2Cl_2$ *and* **3**·C_6H_5Me.—*Crystal data for* **2**. $C_{36}H_{41}B_{11}F_4OP_2PdTe$·$0.89CH_2Cl_2$, M = 1056.2, monoclinic, space group $P2_1/c$, a = 14.073(3), b = 15.640(2), c = 20.262(6) Å, β = 94.80(2)°, D_c = 1.58 g cm^{-3}, U = 4444(2) Å^3, Z = 4, $2\theta_{max}$ = 54°, μ(Mo-Kα) = 12.8 cm^{-1}, λ(Mo-Kα) = 0.701 73 Å, F(000) = 2085, T = 288 K, final R = 0.038, R' = 0.052 (statistical weights, 559 parameters) for 5595 observed reflections.

Crystal data for **3**. $C_{37}H_{39}B_{11}F_4OP_2PdTe$·$C_7H_8$, M = 1082.7, monoclinic, space group $P2_1/c$, a = 14.509(3), b = 10.732(1), c = 31.377(8) Å, β = 97.49(2)°, D_c = 1.49 g cm^{-3}, U = 4844(2) Å^3, Z = 4, $2\theta_{max}$ = 54°, μ(Mo-Kα) = 10.8 cm^{-1}, λ(Mo-Kα) = 0.701 73 Å, F(000) = 2152, T = 293 K, final R = 0.054, R' = 0.071 (statistical weights, 542 parameters) for 5439 observed reflections.

Both compounds were analysed in a similar way (details of data collection and structure determination are summarised in Table 4). Accurate cell dimensions and the crystal orientation matrix were determined by a least-squares refinement of the setting angles of 25 reflections. Data were collected on a CAD-4 diffractometer using graphite-monochromated (Mo-Kα) radiation. The intensities of three reflections measured at 120 min intervals showed no loss in intensity. Lorentz, polarisation and absorption corrections were applied to the data. Both structures were solved using the Patterson heavy-atom method which revealed the positions of the Te and Pd atoms. The remaining non-hydrogen atoms were located in

Table 6 Positional parameters and their estimated standard deviations for compound **3**$\cdot CH_6H_8Me$

Atom	*x*	*y*	*z*	Atom	*x*	*y*	*z*
Te	0.060 59(4)	0.454 41(5)	0.371 77(2)	C(45)	−0.236 8(6)	0.060 6(10)	0.295 0(3)
Pd	0.121 80(4)	0.219 92(5)	0.386 78(2)	C(46)	−0.143 3(6)	0.039 0(8)	0.302 5(3)
P(1)	0.362 32(14)	0.178 32(20)	0.433 38(7)	C(51)	0.028 7(6)	−0.078 9(7)	0.387 8(3)
P(2)	0.033 14(14)	0.054 55(19)	0.352 44(7)	C(52)	0.096 9(6)	−0.098 8(9)	0.422 3(3)
F(1)	0.163 9(6)	0.960 0(7)	0.097 1(3)	C(53)	0.094 4(8)	−0.202 0(9)	0.448 7(3)
F(2)	0.176 4(5)	0.815 1(6)	0.047 2(2)	C(54)	0.023 1(8)	−0.284 2(9)	0.441 5(3)
F(3)	0.042 1(4)	0.914 6(6)	0.051 0(2)	C(55)	−0.044 8(7)	−0.269 1(8)	0.407 2(4)
F(4)	0.159 9(6)	1.014 8(7)	0.028 2(3)	C(56)	−0.042 1(6)	−0.168 4(8)	0.380 7(3)
O	0.052 1(7)	0.164 3(10)	0.471 4(4)	C(61)	0.072 1(6)	−0.011 5(8)	0.305 2(3)
C(1)	0.076 1(7)	0.186 1(10)	0.443 2(3)	C(62)	0.122 7(6)	−0.122 9(8)	0.307 3(3)
C(11)	0.331 3(5)	0.126 0(8)	0.479 8(3)	C(63)	0.159 9(8)	−0.167 8(10)	0.272 3(4)
C(12)	0.278 1(6)	0.214 1(10)	0.506 2(3)	C(64)	0.148 5(8)	−0.103 5(12)	0.233 9(4)
C(13)	0.239 3(7)	0.178 8(11)	0.542 9(3)	C(65)	0.099 0(7)	0.006 1(11)	0.230 4(3)
C(14)	0.234 0(8)	0.055 0(14)	0.552 4(4)	C(66)	0.059 9(6)	0.051 4(8)	0.265 8(3)
C(15)	0.268 8(8)	−0.032 9(11)	0.528 0(4)	C(S1)	0.358 3(13)	1.119 8(19)	0.199 2(6)
C(16)	0.308 0(6)	0.000 6(9)	0.490 8(3)	C(S2)	0.384 8(20)	1.158 0(28)	0.241 5(7)
C(21)	0.467 4(6)	0.260 3(8)	0.455 3(3)	C(S3)	0.444 5(21)	1.084 0(38)	0.269 4(8)
C(22)	0.497 4(7)	0.260 1(9)	0.498 9(3)	C(S4)	0.477 6(16)	0.971 8(34)	0.254 9(11)
C(23)	0.578 2(7)	0.324 4(11)	0.514 9(4)	C(S5)	0.451 1(20)	0.933 6(25)	0.212 6(12)
C(24)	0.628 8(7)	0.385 4(10)	0.486 9(4)	C(S6)	0.391 5(19)	1.007 6(21)	0.184 7(9)
C(25)	0.600 0(7)	0.386 3(10)	0.443 7(4)	C(S7)	0.294 2(16)	1.199 4(23)	0.169 3(8)
C(26)	0.520 3(6)	0.324 1(10)	0.427 6(3)	B	0.136 0(9)	0.927 2(10)	0.055 1(4)
C(31)	0.400 0(6)	0.039 9(8)	0.407 1(3)	B(3)	0.117 3(7)	0.320 5(9)	0.322 5(3)
C(32)	0.492 6(6)	0.007 5(11)	0.410 6(4)	B(4)	0.157 6(8)	0.490 2(9)	0.321 3(4)
C(33)	0.519 2(7)	−0.100 2(12)	0.392 8(4)	B(5)	0.205 6(8)	0.535 6(9)	0.377 6(4)
C(34)	0.453 4(9)	−0.179 4(11)	0.371 1(4)	B(6)	0.201 3(6)	0.393 6(8)	0.415 0(3)
C(35)	0.362 3(8)	−0.147 8(9)	0.366 9(4)	B(7)	0.225 5(6)	0.228 1(8)	0.341 8(3)
C(36)	0.334 7(6)	−0.039 7(8)	0.384 5(3)	B(8)	0.224 5(7)	0.359 8(9)	0.306 7(3)
C(41)	−0.090 3(5)	0.092 3(7)	0.337 0(3)	B(9)	0.277 9(8)	0.490 4(9)	0.338 2(4)
C(42)	−0.131 6(6)	0.169 6(8)	0.363 7(3)	B(10)	0.304 0(6)	0.436 1(8)	0.392 6(3)
C(43)	−0.226 6(6)	0.192 5(9)	0.356 5(3)	B(11)	0.275 4(6)	0.276 1(8)	0.394 7(3)
C(44)	−0.279 5(6)	0.136 5(10)	0.322 2(4)	B(12)	0.319 4(6)	0.337 6(9)	0.348 6(3)

subsequent Fourier synthesis. Hydrogen atoms (visible in difference maps) were included in the refinement at geometrically idealised positions, but restrained to ride on the carbon or boron atom to which they were bonded (C–H 0.95 or B–H 1.08 Å). The hydrogen atoms on the water molecule in compound **2** were also located from difference maps and included in the structure-factor calculation at these positions; no other peaks > 0.3 e Å^{-3} were present near this oxygen atom. Refinement was by full-matrix least squares calculations on *F*, initially with isotropic and later with anisotropic thermal parameters for non-H atoms. In molecule **2** it became obvious during refinement that there was disorder associated with the $[BF_4]^-$ anion which was also involved in hydrogen bonding to the CH_2Cl_2 solvate present in the lattice. There were five fluorine sites, which refined with variable site occupancy to values of 1.0, 1.0, 1.0, 0.6 and 0.4. The boron atoms were disordered over two sites with occupancies of 0.6 and 0.4. The CH_2Cl_2 molecule was disordered over two sites which refined anisotropically to values of 0.53 and 0.36. The disorder was such that the disordered $[BF_4]^-$ anion and CH_2Cl_2 were associated together through hydrogen bonding about an inversion centre. In **3** a difference map calculated at the beginning of the refinement showed that there was a toluene molecule of solvation present in the asymmetric unit. By careful selection of the maxima from a rather diffused electron-density area the positions of the carbon atoms in the toluene molecule were determined.

Scattering factors and anomalous dispersion corrections were taken from ref. 15. All calculations were performed on a Silicon Graphics 4D-380 computer using the NRCVAX programs.[16] Atomic coordinates are given in Tables 5 and 6 for compounds **2** and **3** respectively. Figs. 1 and 3 were prepared using ORTEP II[17] in conjunction with the NRCVAX suite of programs.

Additional material available from the Cambridge Crystallographic Data Centre comprises H-atom coordinates, thermal parameters and remaining bond lengths and angles.

Acknowledgements

A generous loan of palladium salts from Johnson Matthey plc is gratefully acknowledged by T. R. S. G. F. would like to thank the Natural Sciences and Engineering Research Council (Canada) for Grants in Aid of Research.

References

1 Part 11, G. Ferguson, J. F. Gallagher, M. McGrath, J. P. Sheehan, T. R. Spalding and J. D. Kennedy, preceding paper.

2 J. D. Kennedy, *Prog. Inorg. Chem.*, 1984, **32**, 519; 1986, **34**, 211; *Baron Hydride Chemistry*, ed. E. L. Muetterties, Academic Press, New York, 1975; R. N. Grimes, in *Comprehensive Organometallic Chemistry*, ed. G. Wilkinson, Pergamon, Oxford, 1982, vol. 1, 459; L. J. Todd, in *Comprehensive Organometallic Chemistry*, ed. G. Wilkinson, Pergamon, Oxford, 1982, vol. 1, 543.

3 S. G. Shore, J. D. Ragaini, T. Schmitkons, L. Barton, G. Medford and L. Plotkin, *Abstracts 4th Inter. Meeting Boron Chem.*, IMEBORON IV, 1979, Abstract 07.

4 C. J. Jones, J. N. Francis and M. F. Hawthorne, *J. Am. Chem. Soc.*, 1973, **95**, 7633.

5 M. F. Hawthorne, L. F. Warren, K. P. Callahan and N. F. Travers, *J. Am. Chem. Soc.*, 1971, **93**, 2407.

6 H. C. Kang, S. S. Lee, C. B. Knobler and M. F. Hawthorne, *Inorg. Chem.*, 1991, **30**, 2024.

7 A. J. Deeming, I. P. Rothwell, M. B. Hursthouse and L. New, *J. Chem. Soc., Dalton Trans.*, 1978, 1490.

8 P. Castan, J. Jaud, S. Wimmer and F. L. Wimmer, *J. Chem. Soc., Dalton Trans.*, 1991, 1155.

9 M. Grassi, S. V. Meille, A. Musco, R. Pontellini and A. Sironi, *J. Chem. Soc., Dalton Trans.*, 1989, 615.

10 B. P. Andreini, D. B. Dell'Amico, F. Calderazzo and G. Pelizzi, *J. Organomet. Chem.*, 1988, **354**, 369.

11 G. Ferguson, M. Parvez, J. A. MacCurtain, O. Ni Dhubhghaill, T. R. Spalding, X. L. R. Fontaine and J. D. Kennedy, *J. Chem. Soc., Dalton Trans.*, 1987, 699.

12 Faridoon, O. Ni Dhubhghaill, T. R. Spalding, G. Ferguson, B. Kaitner, X. L. R. Fontaine and J. D. Kennedy, *J. Chem. Soc., Dalton Trans.*, 1989, 1657.

13 G. Ferguson, J. D. Kennedy, X. L. R. Fontaine, Faridoon and T. R. Spalding, *J. Chem. Soc., Dalton Trans.*, 1988, 2555.
14 P. Castan, F. Dahan, S. Wimmer and F. L. Wimmer, *J. Chem. Soc., Dalton Trans.*, 1990, 2679.
15 *International Tables for X-Ray Crystallography*, Kynoch Press, Birmingham, 1974, vol. 4.
16 E. J. Gabe, Y. LePage, J.-P. Charland, F. L. Lee and P. S. White, *J. Appl. Crystallogr.*, 1989, **22**, 384.
17 C. K. Johnson, ORTEP II, Report ORNL-5138, Oak Ridge National Laboratory, Oak Ridge, TN, 1976.

Received 7*th July* 1992; *Paper* 2/03570G